ARTICLE

Synthesis and characterization of a new 2-iminothiolate-modified dimethacrylate monomer with potential dental applications

Received 00th January 20xx,
Accepted 00th January 20xx

DOI: 10.1039/x0xx00000x

Rodrigo Pineda Mejía,[†abcd] Luis Fernando Giraldo Morales,[a] John Amalraj,[b] Rodrigo A. Giacaman,[†c*] Leonardo Silva Santos,[†d*]

Supplementary Information

Synthesis and characterization of a new 2-iminothiolate-modified dimethac-rylate monomer with potential dental applications

Rodrigo Pineda Mejía[a, b, c], Rodrigo A. Giacaman[b]*, Luis Fernando Giraldo Morales[c], John Amalraj[d], Leonardo Silva Santos[a]*

[a] Laboratory of Asymmetric Synthesis, Chemistry Institute of Natural Resources, Universidad de Talca, 3460000, Talca, Chile

[b] Cariology Unit, Department of Oral Rehabilitation, Faculty of Dentistry, University of Talca, Talca, Chile

[c] Polymer Research Laboratory, Institute of Chemistry, University of Antioquia, Medellín, Colombia.
[d] Laboratory of Materials Science, Institute of Natural Resources Chemistry, University of Talca, 3460000, Talca, Chile

* Correspondence: lssantos@utalca.cl, giacaman@utalca.cl, ropm04@gmail.com

Supplementary Figures

[a.] *Polymer Research Laboratory, Institute of Chemistry, University of Antioquia, Medellín, Colombia.*
[b.] *Laboratory of Materials Science, Institute of Chemistry of Natural Resources, University of Talca, 3460000, Talca, Chile*
[c.] *Cariology Unit, Department of Oral Rehabilitation, Faculty of Dentistry, University of Talca, Talca, Chile*
[d.] *Laboratory of Asymmetric Synthesis, Institute of Chemistry of Natural Resources, Uni-versidad de Talca, 3460000, Talca, Chile*
† Correspondence: lssantos@utalca.cl, giacaman@utalca.cl, *ropm04@gmail.com*

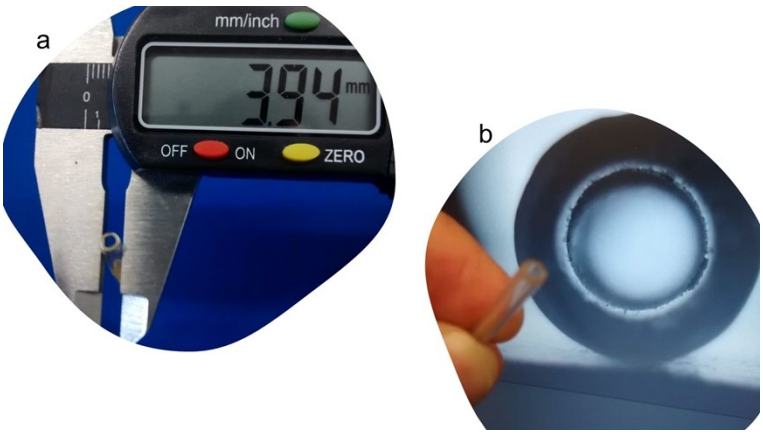

Figure S1. Measurement of capillary diameters.

Image (a) shows the outer diameter of the capillary measured using a digital caliper ($D_{ex}c$). Image (b) shows the external and internal diameters measured using a USB microscope ($D_{ex}m$ and $D_{in}m$, respectively).

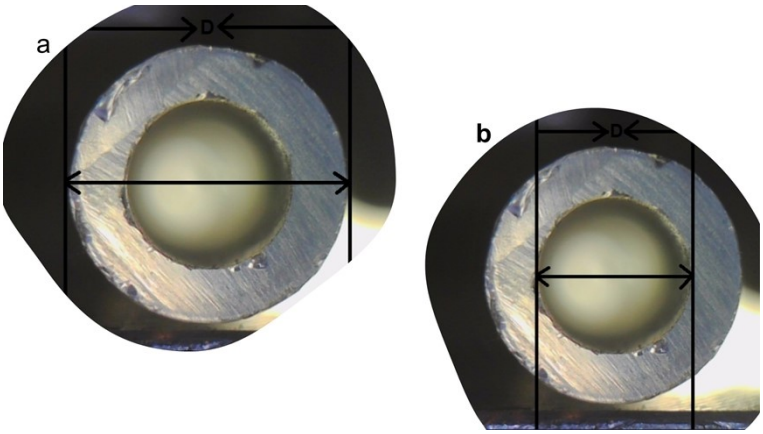

Figure S2. Images acquired using a USB microscope.

Image (a) shows the external diameter of the capillary ($D_{ex}m$), while image (b) shows the internal diameter ($D_{in}m$).

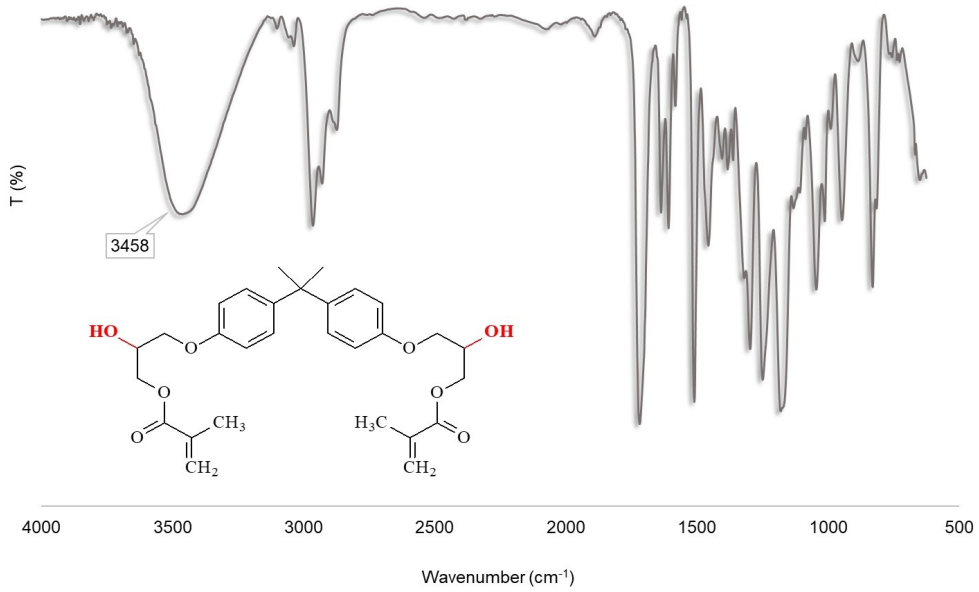

Figure S3. FT-IR spectrum of Bis-GMA. The hydroxyl group (3458 cm^{-1}) is identified, a group that will be replaced.

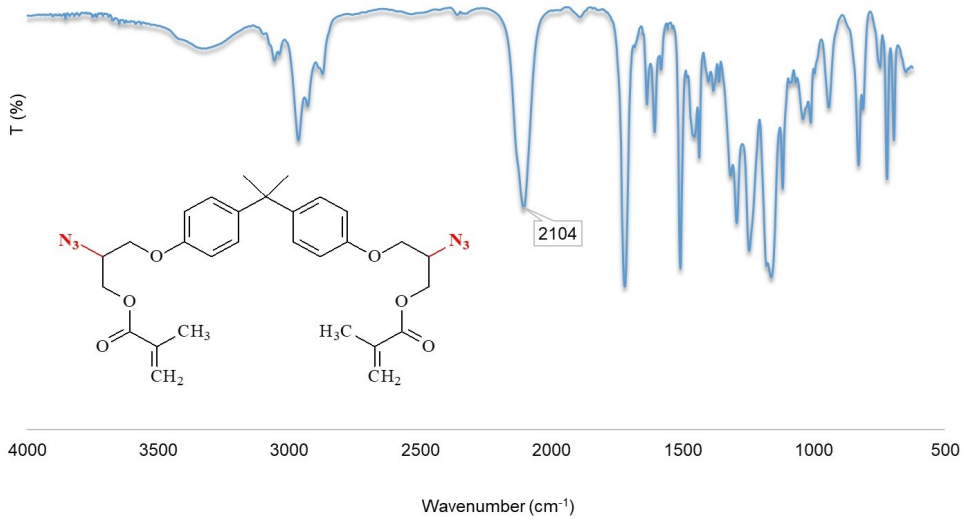

Figure S4. FT-IR spectrum of Bis-GMA.

The hydroxyl (–OH) stretching band is observed at 3458 cm^{-1}, corresponding to the functional group targeted for subsequent chemical modification.

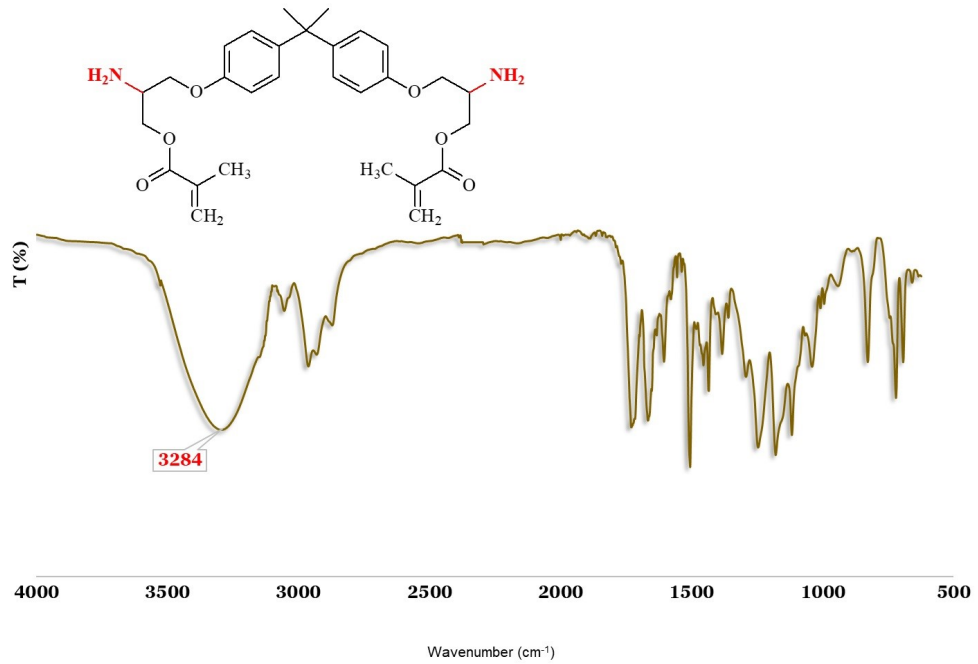

Figure S5. FT-IR spectrum of Bis-[GMA-NH₂].

Following reduction of the azide group, the characteristic absorption band at 2104 cm^{-1} disappears, while a new band at 3284 cm^{-1}, corresponding to N–H stretching of the amine group, is observed.

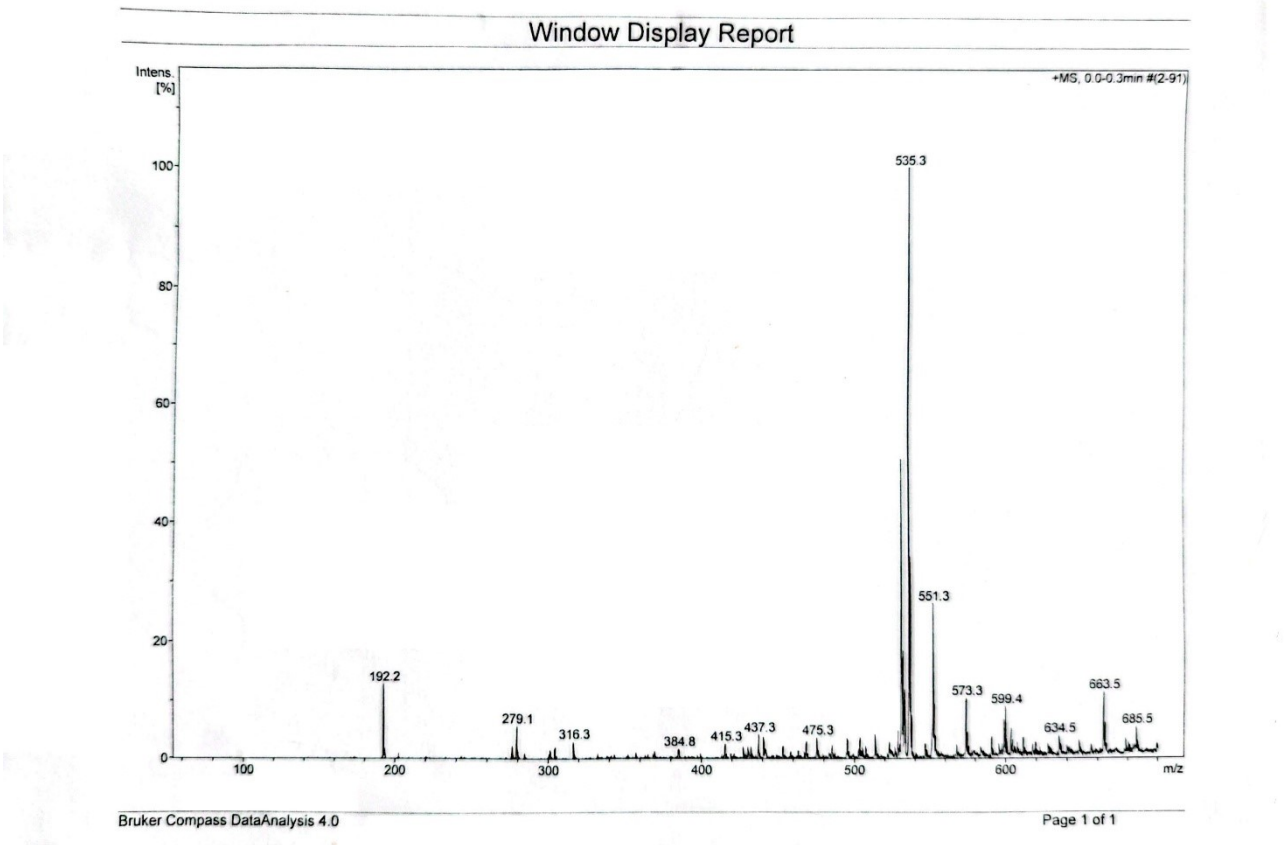

Figure S6. ESI-MS spectrum of Bis-GMA.

The spectrum shows the molecular ion peak at m/z = 535.3, consistent with the expected mass of Bis-GMA, confirming its molecular structure.

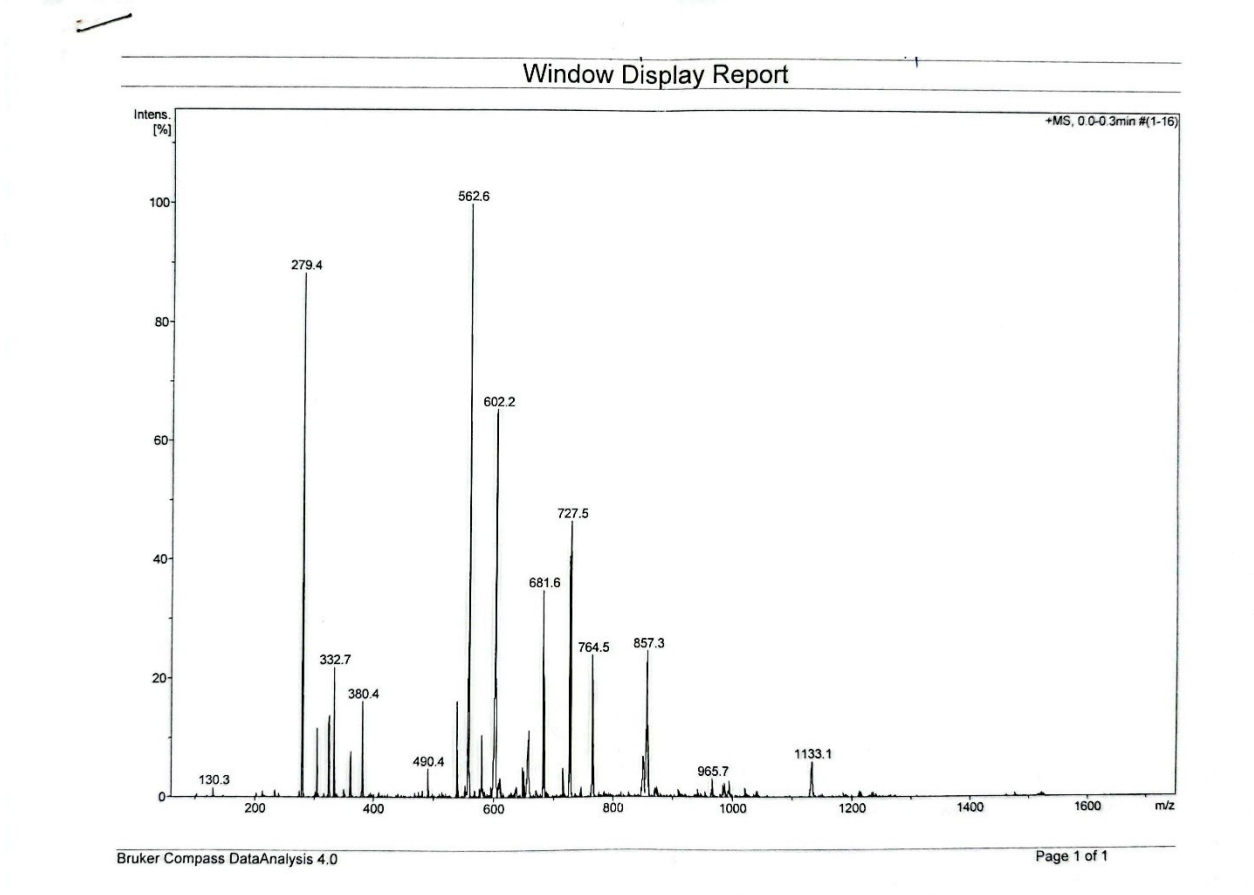

Figure S7. ESI-MS spectrum of Bis-[GMA-N_3].

The spectrum shows the molecular ion peak at m/z = 562.6, consistent with the expected mass of Bis-[GMA-N_3], confirming successful azide functionalization.

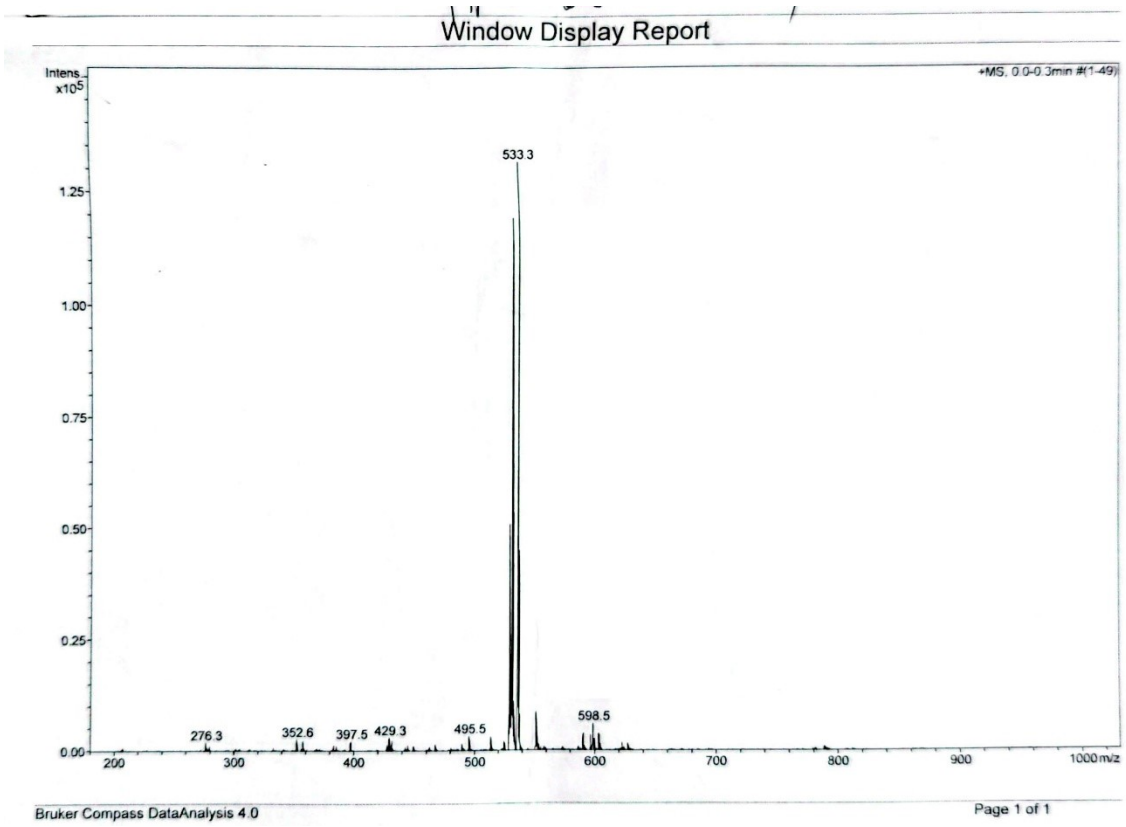

Figure S8. ESI-MS spectrum of Bis-[GMA-NH_2].

The spectrum shows the molecular ion peak at m/z = 533.3, consistent with the expected mass of Bis-[GMA-NH_2], confirming successful azide reduction to amine groups.

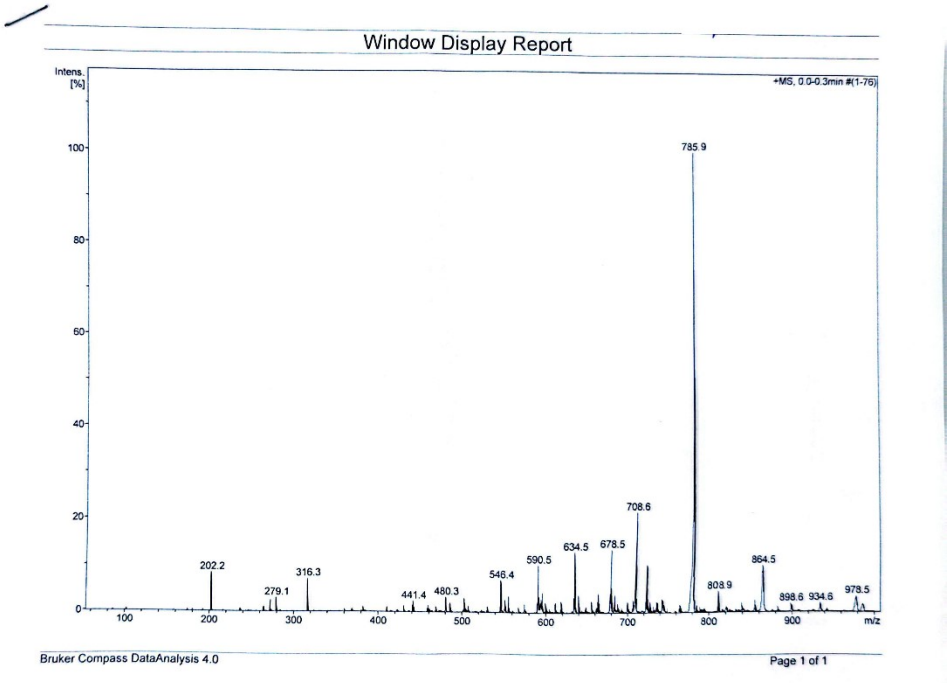

Figure S9. ESI-MS spectrum of Bis-[GMA-TBA].

The spectrum shows the molecular ion peak at m/z = 785.9, consistent with the expected mass of Bis-[GMA-TBA], confirming successful incorporation of the iminothiolane-derived thiol functionality.

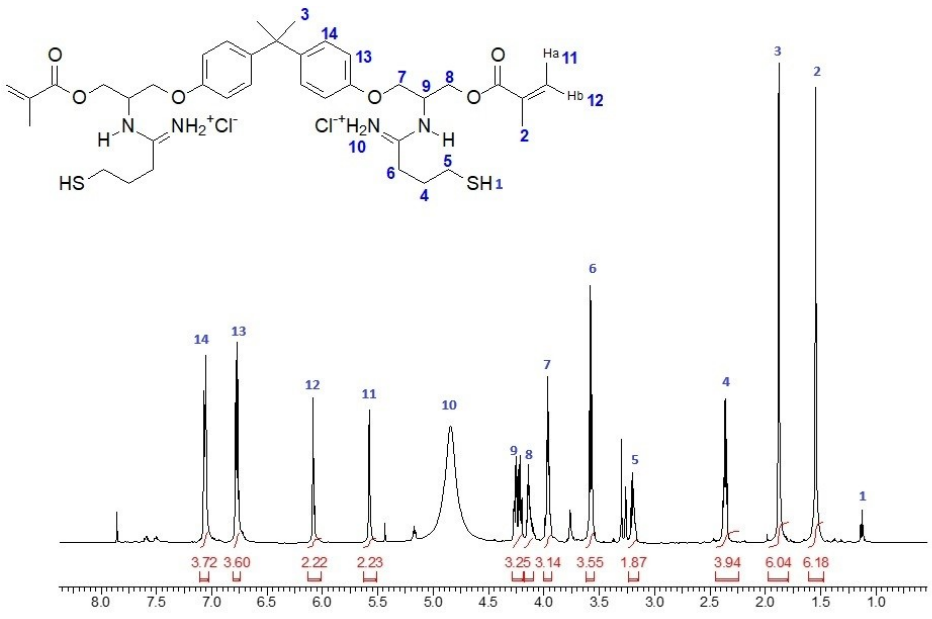

Figure S10. ^{1}H NMR spectrum (600 MHz, CD_3OD) of Bis-[GMA-TBA].

δ 1.20 (t, 1H, –SH), 1.61 and 1.95 (s, 3H, CH_3), 2.40 (m, 2H), 3.40 (m, 2H), 3.63 (t, 2H, CH_2), 4.03–4.35 (m, olefinic and benzylic protons), 4.91 (br s, 1H, amidine), 5.65 and 6.15 (s, 1H, vinyl), 6.84 (d, 2H, J = 7.9 Hz, Ar–H), 7.12 (d, 2H, J = 8.8 Hz, Ar–H).

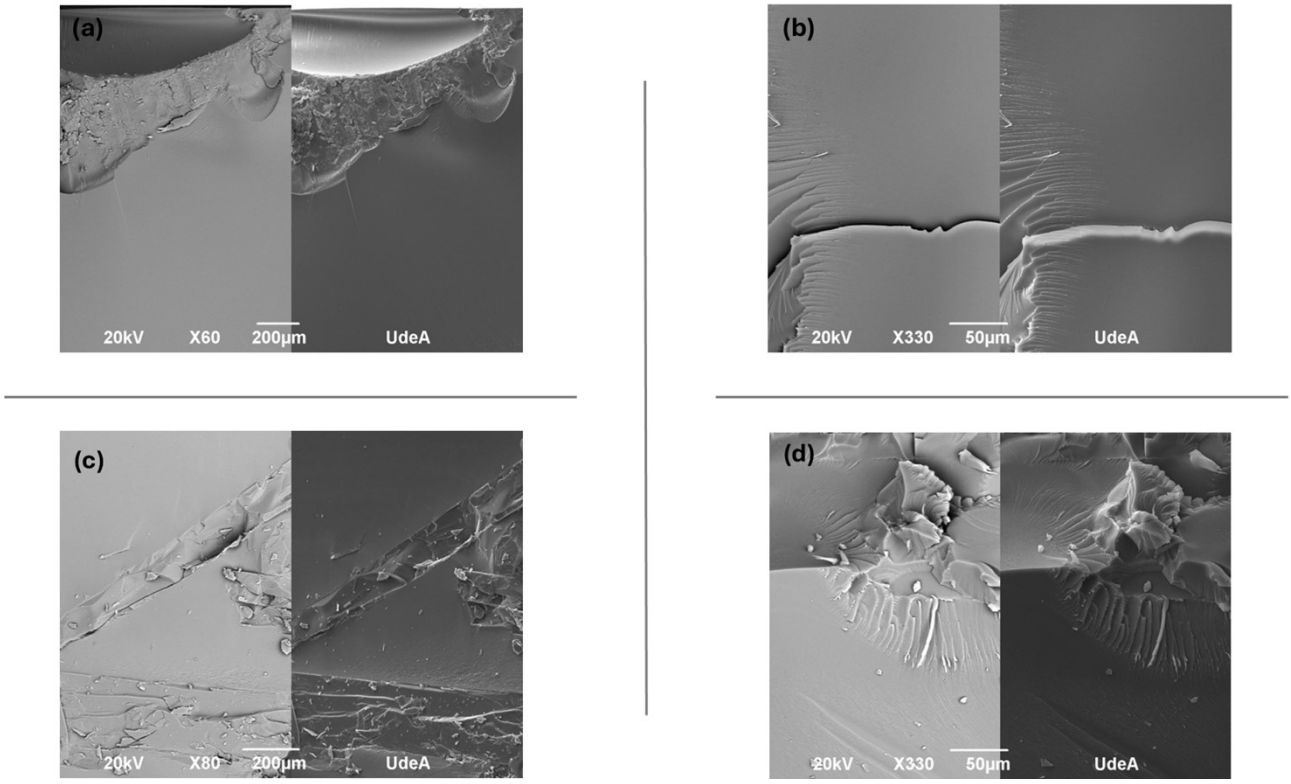

Figure S11. Scanning electron microscopy (SEM) images of GMA50 and TBA50.

Images (a) and (b) correspond to GMA50 at scale bars of 200 µm and 50 µm, respectively, showing a homogeneous morphology. Fracture surfaces appear smooth, with no evidence of particulate debris. Images (c) and (d) correspond to TBA50 at 200 µm and 50 µm, respectively. In contrast, the fracture surfaces exhibit the presence of particulate features, suggesting differences in microstructural organization between the two materials.

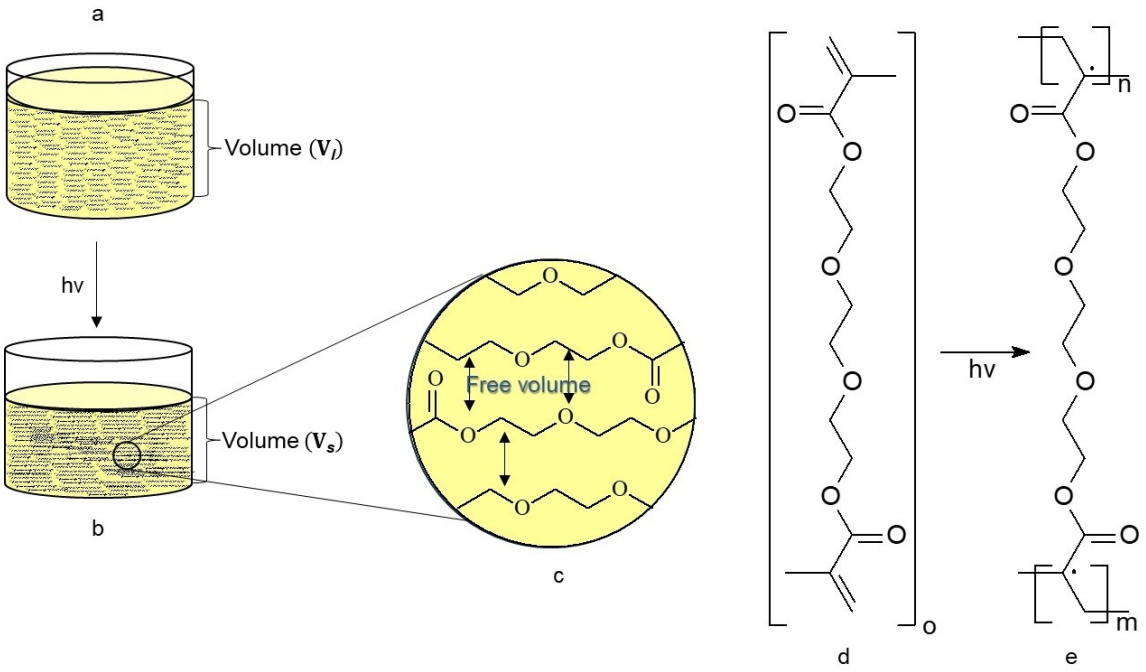

Figure S12. Polymerization of TEGDMA.

Image (a) shows the monomer occupying a given volume in the liquid state. Image (b) shows the polymer after irradiation, occupying a reduced volume in the solid state. In image (c), the polymer chains are more closely packed due to the relatively small size of the pendant groups. Image (d) shows the TEGDMA monomer, and image (e) the corresponding polymer. Following polymerization, a decrease in volume is observed ($V_l > V_s$), corresponding to an experimental volumetric contraction of 13.7% for the TEG99 formulation.

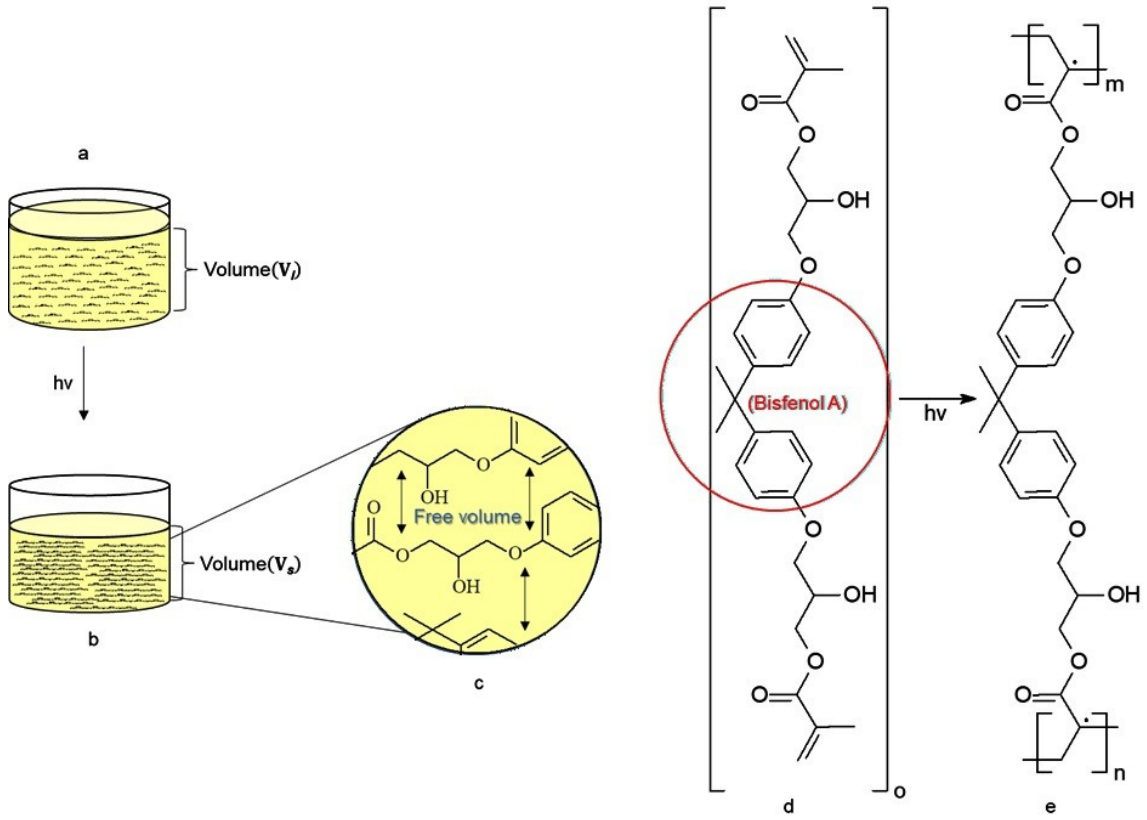

Figure S13. Polymerization of Bis-GMA.

Image (a) shows the monomer occupying a given volume in the liquid state. Image (b) shows the polymer after irradiation, occupying a reduced volume in the solid state. In image (c), the polymer chains are more closely packed due to the relatively lower steric hindrance compared to modified systems. Image (d) shows the Bis-GMA monomer, with the bisphenol A moiety highlighted in a red circle. Image (e) shows the corresponding polymer structure. Following polymerization, a decrease in volume is observed ($V_l > V_s$), corresponding to an experimental volumetric contraction of 11.37% for the GMA50 formulation.

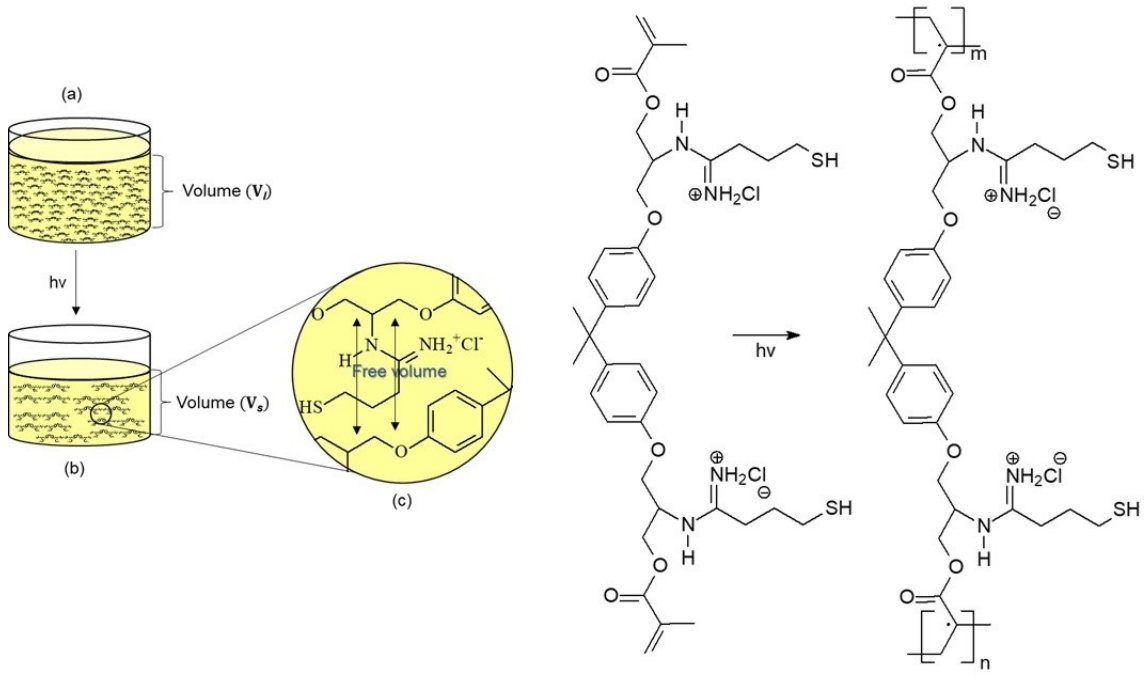

Figure S14. Polymerization of Bis-[GMA-TBA].

Image (a) shows the monomer occupying a given volume in the liquid state. Image (b) shows the polymer after irradiation, occupying a reduced volume in the solid state. In image (c), the polymer chains are more separated due to increased structural rigidity and the presence of bulky pendant groups. Following polymerization, a decrease in volume is observed ($V_l > V_s$), corresponding to an experimental volumetric contraction of 8.5%.

Supplementary Tables

Table S1 Estimated densities of Bis-[GMA-TBA] and Bis-GMA polymers.

$\rho_{poly-[Bis-[GMA-TBA]]} = \frac{1233.8\ kg\ m^3 - (0.5)(1250.0\ kg\ m^3)}{0,5}$	Density poli-[Bis-[GMA-TBA]]
$\rho_{poly-[Bis-[GMA-TBA]]} = 1217.6\ kg\ m^3$	
$\rho_{poly-[Bis-GMA]} = \frac{1237.9\ kg\ m^3 - (0.5)(1250.0\ kg\ m^3)}{0,5}$	Density poly-[Bis-GMA]
$\rho_{poli-[Bis-GMA]} = 1225.8\ kg\ m^3$	

The polymer densities were estimated based on the experimental density of the resin formulations and the known density of poly(TEGDMA).

Table S2 Thermogravimetric analysis (TGA) of GMA50 polymer.

Temperature range of degradation (°C), mass loss (%), and maximum degradation temperature (T_max) determined from the TGA curve.

	Stage 1	Stage 2	Stage 3
°C	25 – 243.21	243.22 – 371.21	371.22 – 625.42
Mass loss (%)	2.20	27.89	62.23
T_max	177.72	352.96	412.02

Table S3 Thermogravimetric analysis (TGA) of TBA50 polymer.

Temperature range of degradation (°C), mass loss (%), and maximum degradation temperature (T_max) determined from the TGA curve.

	Stage 1	Stage 2	Stage 3
°C	25 – 139.83	139.84 -357.00	357.10 – 520.30
Mass loss (%)	1.93	68.43	25.41
T_max	177.66	291.39	387.48

Table S4 Theoretical molar masses of TEGDMA, Bis-GMA, and Bis-[GMA-TBA]

Molecule	Molar Mass (g/mol)	Molecular structure
TEGDMA $C_{14}H_{22}O_6$	286.3	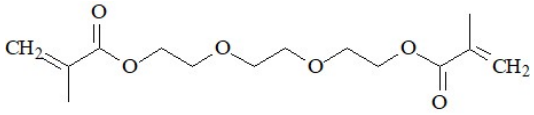
Bis-GMA $C_{29}H_{36}O_8$	512.0	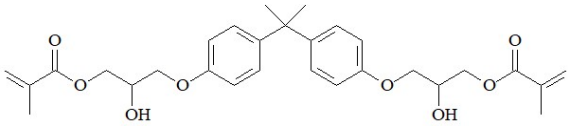
Bis-[GMA-TBA] $C_{37}H_{54}Cl_2N_4O_6S_2$	784.0	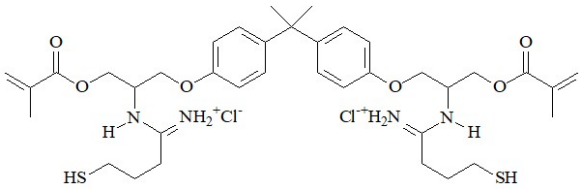

Supplementary Equations

Equations S1. Proportion of external diameters.

$$P = \frac{D_{exm}}{D\bar{e}xc}$$

Equations S2. Estimated inner diameter of the capillary.

$$D_{Ine} = \frac{\bar{D}_{inm}}{\bar{P}}$$

Equations S3. Internal radius of the capillary.

$$R = \frac{D_{Inc}}{2}$$

Equations S4. Volume of liquid resin.

$$V_l = \pi R^2 \bar{A}_l$$

Equations S5. Radius of cylinder.

$$Rc = \frac{\bar{D}_{inm}}{2}$$

Equations S6. Volume of the solid polymer

$$V_s = \pi Rc^2 A_s$$

Equations S7. Percentage of volumetric contraction

$$\%\Delta V = \frac{V_l - V_s}{V_l} 100\%$$

Equations S8. Density estimation

$$\rho_{Blend\ of\ two\ polymers} = (X_{polimer\ 1]})(\rho_{polímer\ 1}) + (X_{polimer\ 2})(\rho_{polímer\ 2})$$

Author Contributions

RP: Conception, design, data acquisition, data analysis and drafting of the first manuscript. LSS, LG and JA: data analysis and critical revision of the manuscript. RAG: Conception, data analysis, editing of the manuscript and critical revision of the manuscript. All authors gave their final approval and agreed to be accountable for all aspects of the work.

Funding

This research received no external funding.

Corresponding author

- Prof. Leonardo Silva Santos, PhD.

1 Poniente 1141, Talca, Chile

Phone: +56-712201547

e-mail: lssantos@utalca.cl

- Prof. Rodrigo A. Giacaman, DDS, PhD.

1 Poniente 1141, Talca, Chile

Phone: +56-712201547

e-mail: giacaman@utalca.cl